



ELSEVIER

Available online at www.sciencedirect.com

SCIENCE @ DIRECT®

Nuclear Instruments and Methods in Physics Research A 514 (2003) 150–155

**NUCLEAR
INSTRUMENTS
& METHODS
IN PHYSICS
RESEARCH**
Section A

www.elsevier.com/locate/nima

Laser detection of radiation enhanced electron transport in ultra-thin oxides

R. Pasternak^{a,*}, Y.V. Shirokaya^a, Z. Marka^a, J.K. Miller^a, S.N. Rashkeev^a, S.T. Pantelides^a, N.H. Tolk^a, B.K. Choi^b, R.D. Schrimpf^b, D.M. Fleetwood^b

^a *Department of Physics and Astronomy, Vanderbilt University, Nashville, TN 37235, USA*

^b *Department of Electrical Engineering and Computer Science, Vanderbilt University, Nashville, TN 37235, USA*

Abstract

Electron transport in a variable-thickness ultra-thin SiO₂-on-Si structure (1.0–6.5 nm) is observed to be enhanced substantially by X-ray radiation-induced damage as detected by a novel fast-pulsed laser technique. This method involves optically stimulated electron injection into the oxide followed by detection of transport, trapping and recombination rates using time-dependent electric-field induced second-harmonic generation (EFISH) arising from charge separation at the interface. This detection technique provides a contactless, noninvasive alternative to electrical characterization.

© 2003 Elsevier B.V. All rights reserved.

PACS: 73.50.Gr; 73.40.Zc; 42.65.Ky

Keywords: Induced leakage current; Thin gate oxides; 2-nd harmonic generation; Silicon

1. Introduction

Recent research in nonlinear optics facilitated by advances in ultra-fast laser technology has shown optical second-harmonic generation (SHG) to be a sensitive probe of buried interfaces [1]. SHG is a contactless and non-destructive technique that can be used to monitor charge-carrier dynamics in ultra-thin oxides. We have found that SHG is a useful tool for in situ measurements that are difficult if not impossible to carry out by conventional electrical probes. As microelectronic

devices decrease in size, oxide thicknesses are drastically reduced. It has been observed that ultra-thin oxides may show a low-field leakage current that can cause performance and reliability problems in MOS devices. These leakage currents can be significantly enhanced by exposure to ionizing radiation [2,3]. The observed enhanced leakage currents can be attributed to an inelastic tunneling process mediated by radiation-induced neutral traps in the oxide [4].

In particular, optical SHG has become an extremely useful technique for surface and interface studies of Si/SiO₂ structures. Crystalline Si is a centrosymmetric material, and thus will not give a SHG signal. But at the Si/SiO₂ interface the symmetry is broken and a SHG signal will result.

*Corresponding author.

E-mail address: robert.pasternak@vanderbilt.edu (R. Pasternak).

In addition, the second-harmonic signal is very sensitive to changes in the magnitude of the electric field across the interface. In the experiment described here, optical SHG detects time-dependent electric fields at the interface arising initially from multi-photon induced injection of electrons in silicon through the interface into the oxide. While most holes remain in the Si close to the interface, electrons are trapped at the oxide surface by the high electron affinity of ambient oxygen molecules. Other types of traps, such as oxide and interface traps, certainly are present, but it was found that for the oxide thickness below 10 nm surface oxide electron traps dominate time-dependent EFISH signal [5]. Electron trapping at the surface results in a charge-separation induced electric field. In the absence of optical excitation these initially surface-trapped electrons may transport across the oxide and recombine with holes on the Si side of the interface, and the measured field is reduced. In this paper we describe recent measurements using a variable thickness SiO₂ layer on silicon in order to focus exclusively on thickness dependence.

2. Experimental methodology

In our experiment we used samples with a Si (100) substrate and an initial SiO₂ oxide thickness of 6.5 nm. The sample was dipped into a 1% solution of hydrofluoric acid at a controlled speed to provide a gradually decreasing thickness of the oxide film [6–8]. A cross-section of the sample is schematically shown in Fig. 1. A Ti:sapphire laser was used for both electron injection and as a probe of interfacial electric field. The laser operated at 800 nm (1.5 eV) with 150 fs pulses, a repetition rate

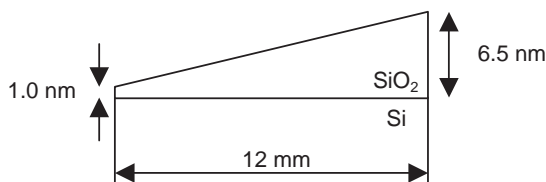


Fig. 1. A cross-sectional view of the sample.

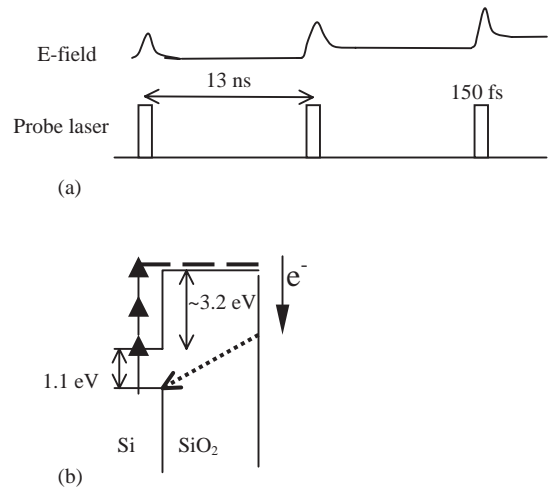


Fig. 2. Schematic diagram of the experiment. (a) Laser pulse timing diagram; (b) electron transfer process within Si/SiO₂ sample.

of 76 MHz, an average power of 250 mW with a spot size diameter of 50 μm .

Fig. 2a schematically shows that the electric field across the interface can increase transiently when a laser pulse hits the sample. This transient behavior has been observed before and was attributed to the separation of electrons and holes in the Si under the influence of an inherent fixed oxide charge [9]. After each laser pulse hits the sample, a small portion of the electrons will cross the interface, transport through the oxide to the surface and be trapped by the ambient surface oxygen. This will result in a cumulative pulse-by-pulse increase in the field across the interface until a steady-state signal is reached. The experimental procedure used in our studies is as follows:

- (1) When laser pulses induce the injection of electrons from Si into the oxide, we observe a rapid increase in the SHG signal due to an increase in the interfacial electric field. This occurs because some of the injected electrons are trapped at the oxide surface, giving rise to a time-dependent electric field at the interface. The electron injection from Si into the oxide is a three-photon process since the difference between the Si valence band and SiO₂ conduction mobility band is approximately 4.3 eV.

(2) After the signal approaches saturation level, we turn on a shutter operating at 0.5 Hz with “on” time of 1/8th s, thus decreasing the duty factor and average power of the laser by a factor of 16. This results in a substantial decrease in electron injection into the oxide, giving rise to a comparably small contribution to the otherwise normally steady electric field over time. As we shall see, the signal, which is a measure of the electric field at the interface, may decrease over time due either to tunneling through a thin sample (less than 3 nm) or to the effects of X-ray irradiation.

One half of the variable thickness Si/SiO₂ sample was irradiated to a 20 Mrad total dose by 10 keV X-ray source at a dose rate of ~ 1 krad(SiO₂)/s. The masked side of the film was not irradiated, and served as a control to help understand the effects of irradiation on charge transport in ultra-thin film SiO₂.

3. Results and discussion

In this paper we report optical second-harmonic measurements to detect and characterize electron transport in radiation damaged and undamaged Si/SiO₂ structures. These measurements were carried out on a single Si/SiO₂ sample with an oxide layer that varied in thickness monotonically from 1.0 to 6.5 nm. This allows us to investigate the thickness dependence of electron transport on an oxide layer with no variation in processing conditions. We observe that, in the unirradiated case, leakage current, which is measured by detecting the reduction in electric field due to tunneling-facilitated transport of electrons across the oxide, became significant only at the smaller thicknesses. However, after radiation exposure the sample showed large leakage currents at all target thicknesses. Standard electrical measurements, such as capacitance–voltage ($C-V$) and current–voltage ($I-V$), are difficult to interpret when the oxide thickness varies in the active device area. We observed similar SHG results in other oxides of comparable thickness, emphasizing the reproducibility of the results [10,11]. Clearly, the optical

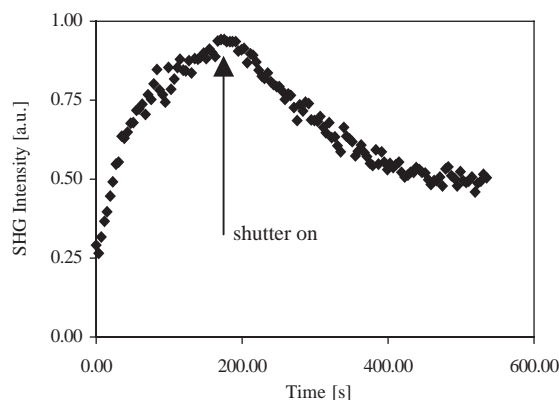


Fig. 3. A time-dependent SHG signal from thick part of the oxide layer taken 20 min after irradiation.

SHG technique, being contactless and non-invasive, can provide important information about carrier transport through ultra-thin oxides.

Fig. 3 shows the data taken 20 min after the sample was irradiated at 20 Mrad at an oxide thickness of ~ 6 nm. The SHG signal begins at a finite level, which implies that there exists a time-independent contribution. The SHG signal is always taken at the same laser peak intensity independent of whether the average beam power is high or low. As discussed above, we control the average power by using a shutter. At a high average beam power, we observed a fast rising SHG signal which approaches a saturation level. At this power level, the laser functions both to inject electrons into the oxide and to measure, by SHG, the resulting increasing field at the interface. After decreasing the average beam power (by turning on the shutter and thus decreasing the duty factor of the laser) we observed a monotonically decreasing SHG signal. We attribute this to a decrease in the electric field, arising from increased transport and subsequent recombination of the surface trapped electrons with holes at the interface due to the effects of X-ray irradiation. For not irradiated thick oxide SHG signal stays at saturation level because the rate of electron tunneling from the surface to the interface is negligible compared to the rate of injection and trapping of electrons. These measurements indicate that the electron transport significantly increases after irradiation. We find that the decay

rate of surface charge in the X-ray irradiated samples is much higher than that of unirradiated samples.

We next show several data fits taken at different times after the sample was irradiated. Each time-dependent data was taken on a different spot of the sample. Fig. 4 represents the data from the thick part of the oxide layer of the sample (approximately 6 nm). On the unirradiated sample, the SHG intensity rose to a steady-state level, and after the beam average power was decreased (by turning on the shutter) the signal remained at the same level indicating little or no electron transport. In contrast, on the X-ray irradiated portion of the sample, after we decreased the average beam power, the signal decreased significantly, indicating an increase in electron transport. Hence, the X-ray radiation-induced defects in the SiO₂ are

seen to greatly enhance conduction current through these thin oxides [10]. Another important observation is that after a significant length of time the irradiation effect begins to disappear and the time-dependent signal approaches the pre-irradiation behavior. Thus the particular defects causing this electron transport are clearly metastable.

Fig. 5 shows the results of measurements performed on a thin part of the sample (approximately 1 nm). On the unirradiated part of the sample, we saw an increase in the signal at high average laser power to a saturation level. On the X-ray irradiated thin portion of the sample, this saturation level was observed to be much lower. When average laser power was decreased, we observed a reduction in the interfacial electric field due to tunneling effects in thin oxides in both unirradiated and irradiated samples. The decrease

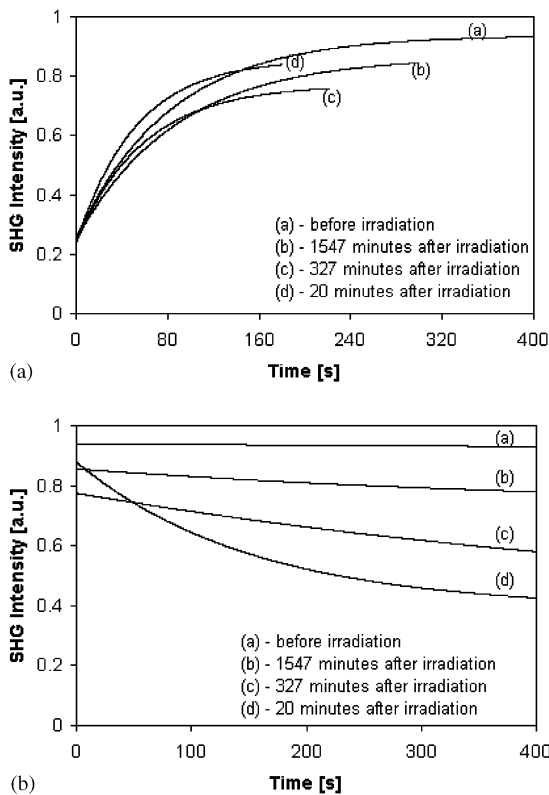


Fig. 4. Exponential fits of time-dependent SHG signals from the thick part of the oxide layer. (a) High average beam power; (b) after the beam power is reduced to a lower average level.

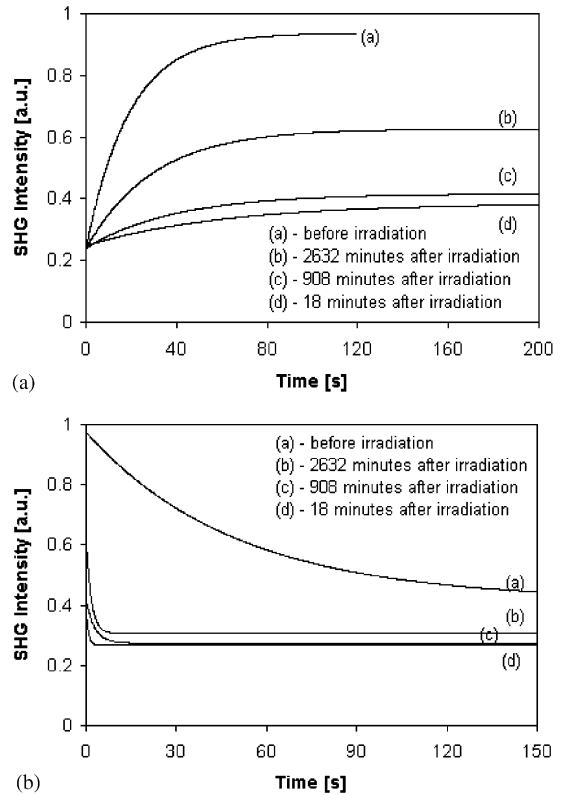


Fig. 5. Exponential fits of time-dependent SHG signals from the thin part of the oxide layer. (a) High average beam power; (b) after the beam power is reduced to a lower average level.

in the photo-induced electric field due to the reduction of the average beam power was much faster in the radiation-damaged sample. This radiation-induced effect, however, decreased with time after irradiation in a similar manner to that observed for the thicker part of the sample.

The experimental results can be explained by the following model.

Time-dependent electric field-induced second-harmonic generation (EFISH) is governed by the following equation:

$$I^{(2\omega)}(t) = |\chi^{(2)} + \chi^{(3)} E(t)|^2 (I^{(\omega)})^2 \quad (1)$$

where $I^{(\omega)}$ and $I^{(2\omega)}(t)$ are the intensities of the fundamental and time-dependent SHG signals, $\chi^{(3)}$ is the third-order nonlinear susceptibility, $\chi^{(2)}$ is the effective second-order susceptibility from all other sources and $E(t)$ is a quasi-static electric field [12]. $E(t)$ is related to the time-dependent oxide surface charge density (which is obtained by integrating the oxide volume charge density over the coordinate perpendicular to the interface), $\sigma(t)$, by

$$E(t) = e\sigma(t)/\varepsilon_{Si}. \quad (2)$$

The main time-dependent contribution to oxide charge density comes from the surface electronic traps due to ambient oxygen described by the following rate equation

$$\frac{dn_e(t)}{dt} = F(t) \frac{n_{0e} - n_e}{\tau_{\text{trap}}} - \frac{n_e}{\tau_{\text{detrapp}}} \quad (3)$$

where n_e is the density of filled electronic surface traps (further we identify $\sigma(t)$ and n_e); n_{0e} is the density of electron surface traps which we assume are initially completely unfilled; $1/\tau_{\text{trap}}$ gives the rate of the trap filling process (related to rate of injection, transport and trapping); and $1/\tau_{\text{detrapp}}$ is the charge dissipation time due to tunneling and subsequent recombination with holes at the interface. The function $F(t)$ is the time-dependent “laser duty factor” (equals to 1 when the shutter is off or 0 when the shutter is on).

When the shutter is off, the steady-state solution (at $t = \infty$) of Eq. (3) is determined by the ratio of τ_{trap} and τ_{detrapp} ,

$$n_e(\infty) = n_{0e} \frac{\tau_{\text{detrapp}}}{\tau_{\text{trap}} + \tau_{\text{detrapp}}}. \quad (4)$$

This is observed in Fig. 5a where steady-state levels are seen to be different at different times after irradiation. Below an oxide thickness of ~ 3 nm electron tunneling and recombination at the interface becomes significant for both irradiated and unirradiated samples [12]. Fig. 5b shows that the pre-irradiation tunneling rate is significantly increased due to X-ray irradiation induced transport.

When the time scale for detrapping is significantly slower than the time scale for trap-filling processes, the time-dependent behavior of the solution of Eq. (3) is totally defined by τ_{trap} (the density exponentially approaches to n_{0e}). This is observed for the thick part of the sample (Fig. 4) before irradiation. For thick samples above approximately 3 nm, the major contribution to the time-dependent EFISH signal is due to charge separation arising from long-lived surface traps. For this case, the rate of electron tunneling from the surface to the interface is negligible compared to the rate of injection and trapping of electrons. Thus only the first term in Eq. (3) needs to be considered for thick samples. The filling process of surface electron traps has an exponential character, what is consistent with our data.

When the shutter is on ($F(t) = 1$), the behavior of the system is defined by the detrapping rate only for all thicknesses, i.e., only the second term of Eq. (3) contributes, and the behavior of n_e is defined by the relaxation rate τ_{detrapp} (the density exponentially relaxes to zero). Fig. 4b shows that these detrapping rates decrease with increasing time after X-ray irradiation.

Our results show that after X-ray irradiation, the oxide is almost transparent to the trapped electrons, which quickly tunnel back through the oxide and recombine with the holes. It has been shown in previous electrical tests that leakage currents can be significantly enhanced after irradiation, due to an inelastic tunneling process mediated by radiation-induced neutral traps in the oxide [2–4]. It was suggested that candidates for these transport-mediating defects are neutral E' centers [13] or they may be hydrogen related [14]. Our data may be explained in a similar manner, i.e. an electron transport mediating mechanism thought to be responsible for radiation-induced

leakage current observed in conventional electrical studies [2–4,8]. The characteristic lifetime of the defects in our radiation damage studies appears to be from several hours to 1–2 days [10,11], suggesting that these transport mediating centers can anneal at room temperature. Previous electrical measurements of radiation-induced leakage current on samples irradiated to much higher doses (125 Mrad (Si)) showed that elevated temperatures (200°C) were required to completely anneal the defects responsible for the observed current leakage [15]. In our experiments the laser should not give rise to any significant heating since we reduced the duty factor of this laser to 1/8th using a shutter. Also, each data point was taken on a fresh spot on the sample, at least 500 μm away from the previous measurement point. With these precautions, we believe laser-heating induced annealing should not be a significant factor in these experiments. This suggests that our laser optical technique is more sensitive to low concentrations of transport mediating defect traps. Alternatively, the defects we observe may be qualitatively different than those observed in electrical measurements at higher doses.

4. Conclusions

In this research, we have demonstrated that second-harmonic generation is a useful technique for the characterization of electron transport in X-ray damaged ultra-thin oxides. Using this technique we have performed time-dependent measurements, which provide dynamical information about injection, trapping, detrapping, transport and recombination processes in thin layers of SiO_2 on Si. In addition, we have shown for the first time that optical SHG measurements can be performed effectively on an oxide sample with a gradually varying thickness (from approximately 1–6.5 nm). The significant differences in carrier-dynamics behavior in thin (~ 1 nm) and thick

(~ 6 nm) oxide layers on the same sample using SHG give unique insight into conventional electron tunneling processes as well as radiation-induced transport mechanisms in thin oxide films.

Acknowledgements

This work was supported by grants from ONR and from AFOSR through the MURI program.

References

- [1] J.F. McGilp, *J. Phys. D: Appl. Phys.* 29 (1996) 1812.
- [2] A. Scarpa, A. Paccagnella, F. Montera, G. Ghibauda, G. Pananakakis, G. Ghidini, P.G. Fuocho, *IEEE Trans. Nucl. Sci.* NS-44 (1997) 1818.
- [3] M. Ceschia, A. Paccagnella, A. Cester, A. Scarpa, G. Ghidini, *IEEE Trans. Nucl. Sci.* NS-45 (1998) 2375.
- [4] L. Larcher, A. Paccagnella, M. Ceschia, G. Ghidini, *IEEE Trans. Nucl. Sci.* NS-46 (1999) 1553.
- [5] J. Bloch, J.G. Mihaychuk, H.M. van Driel, *Phys. Rev. Lett.* 77 (1996) 920.
- [6] S.K. Ghandhi, *VLSI Fabrication Principles*, Wiley, New York, 1994.
- [7] S.A. Campbell, *The Science and Engineering of Microelectronic Fabrication*, Oxford University Press, New York, 2001.
- [8] Y. Takahashi, K. Ohnishi, T. Fujimaki, M. Yoshikawa, M. Page, *IEEE Trans. Nucl. Sci.* NS-46 (1999) 1578.
- [9] J.I. Dadap, P.T. Wilson, H.M. Anderson, M.C. Downer, *Opt. Lett.* 22 (1997) 901.
- [10] Z. Marka, S.K. Singh, W. Wang, S.C. Lee, J. Kavich, B. Glebov, S.N. Rashkeev, A.P. Karmarkar, R.G. Albridge, S.T. Pantelides, R.D. Schrimpf, D.M. Fleetwood, N.H. Tolc, *IEEE Trans. Nucl. Sci.* NS-47 (2000) 2256.
- [11] Z. Marka, R. Pasternak, R.G. Albridge, S.N. Rashkeev, S.T. Pantelides, N.H. Tolc, B.K. Choi, D.M. Fleetwood, R.D. Schrimpf, *J. Appl. Phys.* 93 (4) (2003) 15.
- [12] M.L. Green, E.P. Gusev, R. Degraeve, E.L. Garfunkel, *J. Appl. Phys.* 90 (2001) 2057.
- [13] P.M. Lenahan, J.P. Campbell, A.Y. Kang, S.T. Liu, R.A. Weimer, *IEEE Trans. Nucl. Sci.* NS-48 (2001) 2101.
- [14] P.E. Blöchl, J.H. Stathis, *Phys. Rev. Lett.* 83 (1999) 372.
- [15] P. Riess, M. Ceschia, A. Paccagnella, G. Ghibauda, G. Pananakakis, *Appl. Phys. Lett.* 76 (2000) 1158.